Nanofabrication of optical structures (filters, resonators and sensors)

Frédéric Bedu, Nicolas Bonod, Mireille Commandre, Benjamin Demirdjian, Claude Henry, Artak Karapetyan, Igor Ozerov, Julien Proust, Alain Ranguis, Benjamin Vial

Nanofabrication of optical structures (filters, resonators and sensors)

Frédéric Bedu[1,*], Nicolas Bonod[2], Mireille Commandré[2], Benjamin Demirdjian[1], Claude R. Henry[1], Artak Karapetyan[1], Igor Ozerov[1], Julien Proust[2], Alain Ranguis[1], and Benjamin Vial[2,3]

[1]*Aix-Marseille Université, CNRS, CINAM, UMR 7325, 13288 Marseille, France*

[2]*Aix-Marseille Université, CNRS, Centrale Marseille, Institut Fresnel, UMR 7249, 13013 Marseille, France*

[3]*Silios Technologies, ZI Peynier-Rousset, rue Gaston Imbert Prolongée, 13790 Peynier, France*

[*]*contact author*: bedu@cinam.univ-mrs.fr

Topic : *Lithography, Integration of technologies*

***Abstract* — We fabricated and characterized three types of nanostructures for photonic applications. Gold structures were used for light filtering in the infrared spectral region as well as for molecular sensing based on nanoplasmonics. Also, we fabricated silicon nanostructures showing Mie scattering resonances in the visible and near infrared spectral regions using alkaline etching and gold structures as mask. For all structures, we compare the experimental results vs theoretical modeling.**

I. INTRODUCTION

Nanostructuring of metallic and dielectric surfaces at subwavelength scale can result in spectacular resonant effects. Such structures have recently attracted considerable attention because of their potential applications in integrated photonic components. First, we show the applications of gold structures for light filtering in the infrared spectral region. Second, we apply gold nanoplasmonic arrays for molecular sensing and interaction studies. Third, we fabricated silicon nanostructures featuring Mie scattering resonances in the visible and near infrared spectral regions using gold structures as mask. We will give a comparison between modeling and experiments, mostly obtained by optical spectroscopy. All nanostructures were obtained in our clean room facilities using nanofabrication tools such as electron beam lithography, magnetron sputtering or thermal evaporation and chemical or reactive ion etching.

II. REALISATION

A. *Infrared filter.*

Infrared filters are based on square annular aperture arrays (AAAs) in a thin gold film (Fig. 1). The optical properties of the filters depend on interior and exterior widths of apertures [1,2]. We tuned the central wavelength of the filter transmission in the range of 7–12 μm, by varying the aperture width and pitch. The results of the Finite Element Method (FEM) simulations are summarized in table 1 and shown in fig 1a. The geometry of the features is shown in the inset of fig. 1a.

Filter	Λr, μm	d, nm	w1, nm	w2, nm
M1	8	1920	850	1060
M2	9.7	2250	990	1240
M3	10.3	2600	1140	1430
M4	12	2930	1290	1610

Table 1: Results of the Finite Element Method (FEM) simulations: λr - central wavelength; d – array pitch; w1 and w2 - interior and exterior widths of apertures.

Samples with the aforementioned parameters have been fabricated on the same double side polished (100) pure intrinsic silicon substrate. The nanostructuring has been performed by electronic beam lithography (EBL) using a lift-off process with a negative resist. A relatively large area of 3×3mm2 has been nanostructured for each of the four samples to allow the measurements of FTIR spectra.

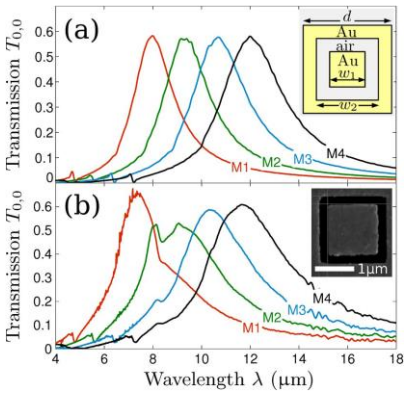

Fig. 1. Transmission spectra at normal incidence in the specular order T0,0 as a function of incident wavelength λ for the different filters. (a) FEM simulations for the filters denoted M1,M2,M3,M4 respectively: central wavelength λr = 8, 9.7, 10.3 and 12 μm. The geometry of the features is shown in the inset. (b) FTIR measurements. The inset shows a typical SEM image of an individual filter.

The measured spectra at normal incidence and in TM polarization are reported in Fig.1b and show good agreement with the numerical simulations, even if the experimental resonances are slightly blue-shifted and broader because of variations on the fabricated aperture widths.

B. *Indirect nanoplasmonic sensor.*

The second type of structures we fabricated and studied is also based on plasmonics in metals. We used localized surface plasmon resonance (LSPR) in gold nanodisks to create a nanosensor array to study the interaction of water vapors with aircraft engine soot nanoparticles [3]. LSPR is very sensitive to small local changes in refractive index at the surface of metal nanostructures during the adsorption/desorption of molecules. These changes induce a shift in the wavelength of the optical LSPR response, and the gold nanodisks act individually as nanodetectors of the reactivity of water with deposited soot nanoparticles.

Gold nanodisks were fabricated by EBL (electron beam lithography) on a borosilicate glass window via a "lift-off process" with a positive e-beam resist. The glass window presents a quite large nanostructured surface of 720 x 720 µm2 with gold nanodisks having a typical in-plane diameter of ~100 nm. The EBL technique allows to control precisely the size and distance between the gold nanodisks. Then we have deposited a thin SiO_2 layer of about 10 nm on gold nanodisks by RF magnetron sputtering. Fig. 2 shows a typical atomic force microscopy (AFM) image of the soot particles deposited on gold nanodisk arrays covered by a SiO_2 layer.

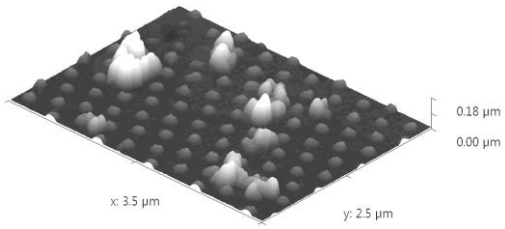

Fig. 2. Tapping mode topographical AFM image of AEC soot particles deposited on gold nanodisks (covered by a SiO2 layer). Image obtained with a PSIA apparatus (XE-100).

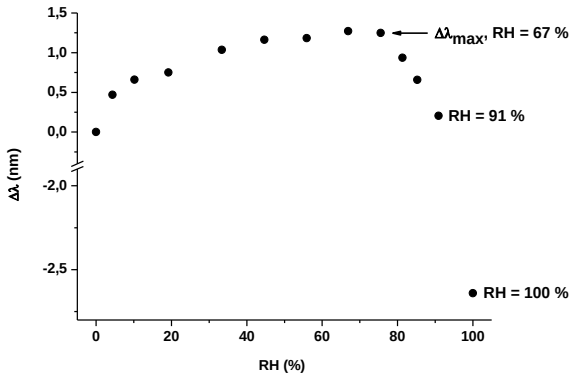

Fig. 3. Evolution of the shift of the LSPR maxima signal vs the relative humidity of the reactor (at room temperature) during the adsorption of water vapor on AEC soot particles deposited on gold nanodisks (+ SiO2 layer).

To measure the LSPR response we used an experimental device wherein the sample fits into an UHV stainless steel reactor equipped with a controlled water vapor injection system and two transparent windows for transmission measurements. The optical signal transmitted by the sample is collected and analyzed in the 360-900 nm spectral range by a UV-VIS spectrometer.

We varied the relative humidity (RH) inside the reactor at room temperature in a full range from 0 to 100%. Fig. 3 shows the shift of the spectral position ($\Delta\lambda$) of the LSPR response during the adsorption of water vapor on the SiO_2 covered gold nanodisks. We observed a non-linear variation of the signal and a blue shift (negative $\Delta\lambda$) in the presence of aircraft engine combustor (AEC) soot on nanosensor arrays. The changes in the slope of $\Delta\lambda$ at *RH* = 67 % and *RH* = 91% shown in fig. 3 indicate that the optical properties of soot particles are modified. On the contrary, for bare nanostructures without soot particles, we observed only a linear red shift with respect to the relative humidity. A theoretical model is proposed to explain such a behavior.

Finally, the LSPR-based structures can be adapted for sensing other molecules, not only water, and can also be used in catalysis monitoring.

C. *Silicon optical resonators*

Contrary to the two previous examples, here we use a dielectric/semiconductor material (silicon) and not metallic layer to make optical resonators [4]. High resolution nanostructures were patterned by EBL on a resist layer. Then the features were transferred by lift-off technique on a gold layer used in this case only to mask the surfaces of amorphous and crystalline silicon in alkaline solutions (potassium or tetramethylammonium hydroxide) during chemical etching. The sketch of the fabrication process is shown in fig. 4. At the final step, the gold mask is chemically removed.

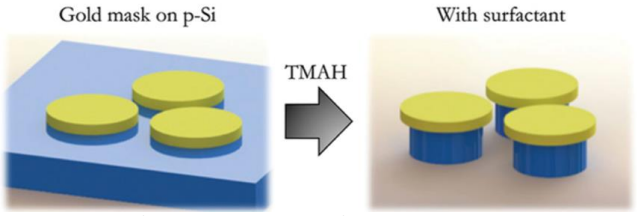

Fig. 4 Sketch of the silicon nanopillar fabrication process by alkaline wet etching.

The shape of typical individual nanostructures was cylindrical with a height of 300 nm. After numerical optimization of the resonator geometry, we chose the diameter of nanopillars from 160 to 195 nm in order to observe the electric and magnetic dipolar resonances in the visible optical range.

The results of optical characterization by forward scattering on typical patterns and simulated spectra are shown in fig. 5. Four spectral peaks are clearly observed for each pillar diameter. We identified each resonance type and indicated them in fig. 5 by MD for magnetic dipolar resonance, ED for electric dipolar resonance, MQ for magnetic quadrupolar resonance, and EQ for

electric quadrupolar resonance. When increasing/decreasing the pillar diameter, all resonance peaks shifted to the blue/red spectra in accordance with theoretical simulations.

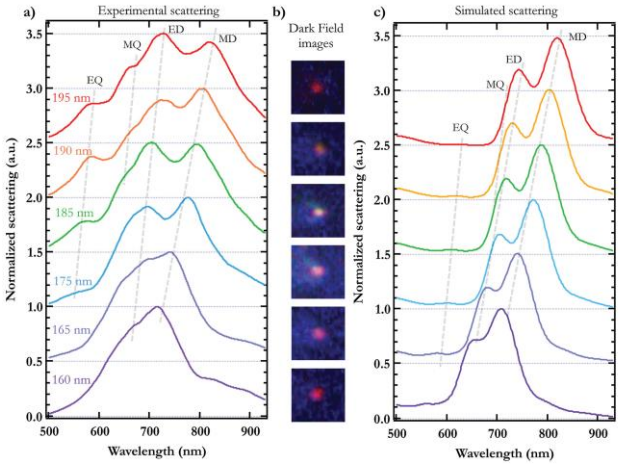

Figure 5. a) Normalized experimental forward scattering spectra of six nanoparticles with diameters ranging between 160 and 195 nm (thickness of 300 nm). The spectra are stacked one above the other. The diameter includes the oxide layer of thickness 5 nm. b) Dark field images in transmission of each resonator. c) Numerical simulations of cylinders with the oxide layer.

ACKNOWLEDGMENT

We thank Stéphane Chenot, Ibrahima Soumahoro and Bruno Gallas (Institut des Nanosciences de Paris) for deposition and optical characterisation of thin silicon films; Redha Abdeddaim (Institut Fresnel) for his help with simulations of dielectric scattering, and Hervé Dallaporta (CINaM) for fruitful discussions on infrared filter fabrication.

Nanofabrication processes were performed in Planète CT-PACA clean room facility.

REFERENCES

[1] B. Vial, M. Commandré, G. Demésy, A. Nicolet, F. Zolla, F. Bedu, H. Dallaporta, S. Tisserand, and L. Roux, "Transmission enhancement through square coaxial aperture arrays in metallic film: when leaky modes filter infrared light for multispectral imaging," Optic Letters, vol. 39, pp. 4723-4726, 2014.

[2] M. Commandré, B. Vial, S. Tisserand, L. Roux, H. Dallaporta, F. Bedu, G. Demésy, A. Nicolet, and F. Zolla, "Design, fabrication and characterization of resonant metamaterial filters for infrared multispectral imaging," Thin Solid Films, in press, 2015.

[3] B. Demirdjian, F. Bedu, A. Ranguis, I. Ozerov, A. Karapetyan, and C.R. Henry, "Indirect nanoplasmonic sensing to probe with a high sensitivity the interaction of atmospheric water with soot aerosols," The Journal of Physical Chemistry Letters, in press, 2015. DOI: 10.1021/acs.jpclett.5b01630

[4] J. Proust, F. Bedu, S. Chenot, I. Soumahoro, I. Ozerov, B. Gallas, R. Abdeddaim, and N. Bonod, "Chemical alkaline etching of silicon Mie particles," Advanced Optical Materials, vol. 3, pp. 1280-1286, September 2015.